Green Chemistry

PAPER

View Article Online
View Journal | View Issue

Cite this: *Green Chem.*, 2024, **26**, 9911

Increasing the diversity of nylonases for poly(ester amide) degradation†

Jan de Witt, [a] Maike-Elisa Ostheller,[b] Kenneth Jensen, [c] Christian A. M. R. van Slagmaat, [d] Tino Polen, [a] Gunnar Seide,[b] Stephan Thies, [a] Benedikt Wynands [a] and Nick Wierckx [a]*

Global production of synthetic polyamides (PA), or nylons, is increasing while recycling rates are currently below 5% contributing to the global plastics crisis. Enzymatic depolymerization is a powerful strategy to overcome the drawbacks of mechanical and chemical recycling and has the potential to increase PA recycling rates. However, enzymatic depolymerization of PA is currently limited to a small group of nylonases (NylC) that exhibit low activities making them unsuitable for efficient enzymatic recycling. In this study, we extend the diversity of nylonases, namely $NylC_1$, $NylC_2$, and $NylC_3$ by library screenings and *in silico* analysis. Three novel nylonases were identified that showed varying sequence identities ranging from 84 to 32% compared to the previously characterized $NylC_{p2}$ from *Paenarthrobacter ureafaciens*. Activity of these nylonase candidates towards cyclic PA-oligomers was confirmed *via* the detection of soluble degradation products. These nylonases were also active on synthesized poly(ester amides) (PEA), and this activity was synergistically increased by combination with the leaf and branch compost cutinase LCC resulting in the hydrolysis of approximately 1% of the total polymer. Overall, our discoveries greatly increase the sequence space of NylC enzymes for future enzyme engineering strategies to boost their activities, and they show the potential of PEA for tuning the biodegradability of performance polymers. Thereby, this study leads the path for developing efficient enzymatic PA and PEA depolymerization processes, revealing significant insights into combining the contrary parameters of performance and biodegradability of polymers.

Received 5th April 2024,
Accepted 5th August 2024

DOI: 10.1039/d4gc01662a

rsc.li/greenchem

1 Introduction

Synthetic polyamides (PA), or nylons, are characterized by their durability and high tensile strength, leading to their widespread application in the textile, fishing gear, and automotive industry. Polycaprolactam (PA6) and poly(hexamethylene adipamide) (PA6.6) are the most industrially relevant PA and are obtained by ring-opening polymerization of ε-caprolactam, that is the lactam of 6-aminohexanoate (Ahx), and polycondensation of adipic acid and 1,6-hexamethylenediamine, respectively. Despite an increasing production, PA recycling rates are below 5% contributing to the global plastics crisis as the majority of post-consumer PA is landfilled.[1,2] The mostly linear cradle-to-grave lifespan of PA can be explained by the limitations of traditional recycling strategies. Mechanical recycling, performed by melting and re-extrusion, typically requires highly pure feedstocks while yielding reduced-quality products.[3] Consequently, the materials undergo downcycling that ultimately leads to their disposal. Chemical recycling, on the contrary, depolymerizes the material into its monomers and oligomers, which can then be purified and re-polymerized thereby maintaining the material's properties. However, chemical depolymerization, such as for PA6, typically requires high amounts of energy as well as expensive and often non-recyclable catalysts while being sensitive towards feedstock contaminations.[4] Contrary to this, enzymatic depolymerization displays a sustainable solution for the breakdown of plastics as enzymes operate at moderate conditions compared to chemical processes, catalyze selective reactions, and avoid toxic chemicals.[5] For poly(ethylene terephthalate) (PET), enzymatic recycling is advancing towards commercial implementation due to the design of tailored PETase variants.[6–8] Moreover, techno-economic analyses predict that enzymatic recycling could become cost-competitive with virgin PET production if key cost drivers can be reduced.[9,10] Recent approaches also focused on combining chemical hydro-

[a]*Institute of Bio- and Geosciences IBG-1: Biotechnology, Forschungszentrum Jülich, Jülich, Germany. E-mail: n.wierckx@fz-juelich.de*
[b]*Aachen-Maastricht Institute for Biobased Materials (AMIBM), Maastricht University, Brightlands Chemelot Campus, Urmonderbaan 22, 6167 RD Geleen, The Netherlands*
[c]*Novonesis A/S, Biologiens Vej 2, Kgs. Lyngby DK-2800, Denmark*
[d]*B4Plastics BV, IQ-parklaan 2A, 3650 Dilsen-Stokkem, Belgium*
† Electronic supplementary information (ESI) available. See DOI: https://doi.org/10.1039/d4gc01662a

lysis with biological catalysis, which allows metabolic funneling of mixed hydrolysates and subsequent upcycling to value-added products using engineered microorganisms. Such hybrid strategies were successfully demonstrated for PET[11] and PA (de Witt *et al.*, manuscript in preparation).

Although natural PAs are ubiquitous in nature, such as in proteins or silk, enzymatic depolymerization of synthetic PAs is rare. In fact, only a small group of 6-aminohexanoate-oligomer hydrolases, designated as nylonases, is reported to hydrolyze the amide bonds of synthetic PA6 oligomers. The Ahx-cyclic-dimer hydrolase (NylA – EC 3.5.2.12) specifically converts the cyclic Ahx-dimer (Ahx_2) into linear Ahx_2.[12] NylB (EC 3.5.1.46) acts as Ahx-oligomer exohydrolase and degrades linear Ahx-oligomers by an *exo*-type mechanism resulting in the sequential release of Ahx.[13] The third nylonase, NylC (EC 3.5.1.117), is an Ahx-oligomer endohydrolase and degrades both cyclic and linear Ahx-oligomers with a degree of oligomerization greater than three.[14] All three nylonases ($NylA_{p2}$, $NylB_{p2}$, and $NylC_{p2}$) were discovered on plasmid pOAD2 in *Paenarthrobacter ureafaciens* that was isolated from wastewater of a PA-manufacturing plant.[15,16] Interestingly, activity of nylonases is limited towards synthetic Ahx-oligomers while no activity was reported to a variety of natural amides.[13,17]

NylC is the most promising nylonase for PA depolymerization due to its endo-cleavage mechanism and specificity for larger Ahx-oligomers. Initially, NylC is expressed as inactive precursor protein. After post-translational auto-cleavage between N266 and T267, which results in the formation of an α-(27.4 kDa) and β-subunit (9.4 kDa), structural re-assembly generates an active NylC enzyme.[18] Based on this characteristic, NylC is classified as a member of the N-terminal nucleophile-(N-tn) hydrolase superfamily. Besides the D308-D306-T267 catalytic triad, NylC also possesses Y146 and K189 as additional catalytic or substrate-binding residues that are required for substrate hydrolysis.[19] Although $NylC_{p2}$ is able to degrade linear Ahx-oligomers ($n > 2$), the wild type enzyme shows negligible activity towards PA6.[19] Enzyme engineering of $NylC_{p2}$ resulted in a quadruple mutant that showed increased thermostability and exhibited catalytic activity towards powdered and thin-layered PA6, PA6.6, and PA6.6-*co*-6.4.[20,21] Recently, the activity of this mutant was further increased by directed evolution.[22] Two highly similar homologs of $NylC_{p2}$ were identified in *Agromyces* sp. KY5R ($NylC_A$) and *Kocuria* sp. ($NylC_K$) that share 98.6 and 95.8% sequence identity towards $NylC_{p2}$.[23] Until today, only a limited number of nylonases including the three highly similar NylCs were characterized in literature.[24] This limited enzymological diversity severely hinders the potential of enzymatic PA depolymerization, especially with regard to machine learning-aided engineering.[25]

In this study, we aimed to increase the diversity of characterized NylCs with activities towards PA-related substrates including the emerging group of poly(ester amides) (PEA). The latter group gains increasing interest in the polymer industry as it combines the mechanical properties of PA with the biodegradability of polyester.[26] Although PEA market volume is still relatively small, emerging polymers should be developed with their end-of-life options in mind, especially for complex polymers that contain multiple monomers. To identify novel NylC candidates, library screenings and *in silico* analyses were performed. NylC candidates were expressed in *Bacillus* sp. and subjected to activity assays using Ahx-oligomers and polymers. This study greatly increases the enzymological diversity of NylCs, thereby facilitating future enzyme engineering efforts for the development of enzymatic PA recycling processes. Further, combined enzymatic degradation and architectural design of PEA provide key insights into polymer design that allow the alignment of both biodegradability and performance, which often are opposing polymer features. This study thus facilitates the development of bio-upcycling processes in an integrated manner, enabling a shift towards a more circular plastics economy.

2 Results and discussion

2.1 Screening and expression of novel NylC candidates

To increase the diversity of NylCs, public and internal databases were screened for homologs of $NylC_{p2}$[14] (UniProt: Q79F77). We also performed enrichment cultures of compost samples using PEA to isolate strains with putative nylonase activities. This led to the isolation of a *Rhodococcus* sp. and a *Gordonia* sp. as revealed by 16S rDNA analysis and subsequent whole-genome sequencing (Fig. S1†). Since the characterized $NylC_{p2}$, $NylC_A$, and $NylC_K$ are closely related, we screened the obtained datasets *in silico* for NylC candidates with different amino acid sequences towards $NylC_{p2}$ to yield a diverse set of enzyme candidates. Apart from $NylC_{p2}$, six NylC candidates ($NylC_{1-6}$) were successfully expressed and purified, each with varying amino acid sequence identities compared to $NylC_{p2}$ (Table 1 and Fig. 1). Multiple sequence alignments revealed the presence of the typical N/T autocleavage site in all NylC candidates classifying them into the N-tn hydrolase superfamily (Fig. 1). Moreover, the D308-D306-T267 catalytic triad of $NylC_{p2}$ was highly conserved in $NylC_{1-6}$ (Table 1 and Fig. 1). $NylC_{1-4}$ also possessed the two additional catalytic residues, namely Y148/Y130/Y137/Y120 and K191/K173/K180/K163, required for PA hydrolysis as revealed for $NylC_{p2}$. In $NylC_5$ and $NylC_6$, these additional catalytic residues were less conserved since Y146 was replaced by F130/F129 and no K could be identified corresponding to position K189 of $NylC_{p2}$ by multiple sequence alignments. Using ColabFold,[27] the structures of $NylC_{1-6}$ were predicted and aligned to $NylC_{p2}$. These structural alignments revealed that K244 of $NylC_6$ and K189 of $NylC_{p2}$ were in close proximity indicating that $NylC_6$ potentially harbors all catalytic residues required for PA hydrolysis. Although $NylC_5$ contained K242, structural alignments indicated an incorrect arrangement of this residue as it was opposed to K189 of $NylC_{p2}$ (Fig. 2). Overall, structural alignments revealed that the catalytic triads are highly conserved in all NylC candidates compared to $NylC_{p2}$ (Fig. 2, Fig. S2 and Table S2†). Moreover, $NylC_5$ and $NylC_6$ differ from $NylC_{1-4}$, as the additional catalytic residues were less conserved, which might influence their activity towards PA.

Table 1 Overview of NylC enzymes. The amino acid sequence identity towards $NylC_{p2}$ is shown as well as the predicted molecular weight of the α- and β-subunit upon post-translational autocleavage with C-terminal His_6-tag. Multiple sequence alignments and structural alignments indicated the putative catalytic triads of $NylC_{1-6}$. The melting temperature (T_m) of purified $NylC_{1-6}$ was determined by nano differential scanning fluorimetry. Sequences of $NylC_{1-6}$ are shown in Table S1†

Protein ID	Donor organism	Sequence identity (%)	Molecular weight (α + β) (kDa)	Putative catalytic triad	T_m (°C)	Ref.
$NylC_{p2}$	*Paenarthrobacter ureafaciens*	100	27.4 + 9.4	D308, D306, T267	52	Kinoshita *et al.*[13]
$NylC_A$	*Agromyces* sp. KY5R	98.6	27.4 + 9.4	D308, D306, T267	60	Yasuhira *et al.*[23]
$NylC_K$	*Kocuria* sp.	95.8	27.4 + 9.4	D308, D306, T267	67	Yasuhira *et al.*[23]
$NylC_1$	*Leucobacter chromiiresistens* JG 31	84.2	28.0 + 10.4	D310, D308, T269	58.4	This study
$NylC_2$	*Microbacterium oxydans*	62.5	26.0 + 10.2	D292, D290, T251	67.4	This study
$NylC_3$	*Streptomyces* sp. 63005	61.2	26.4 + 10.2	D298, D296, T257	63.9	This study
$NylC_4$	*Variovorax boronicumulans*	48.4	25.9 + 9.3	D292, D290, T251	82.9	This study
$NylC_5$	*Gordonia* sp.	31.7	24.3 + 12.6	D289, D287, T248	78.1	This study
$NylC_6$	*Rhodococcus* sp.	30.0	25.1 + 11.7	D291, D289, T250	74.9	This study

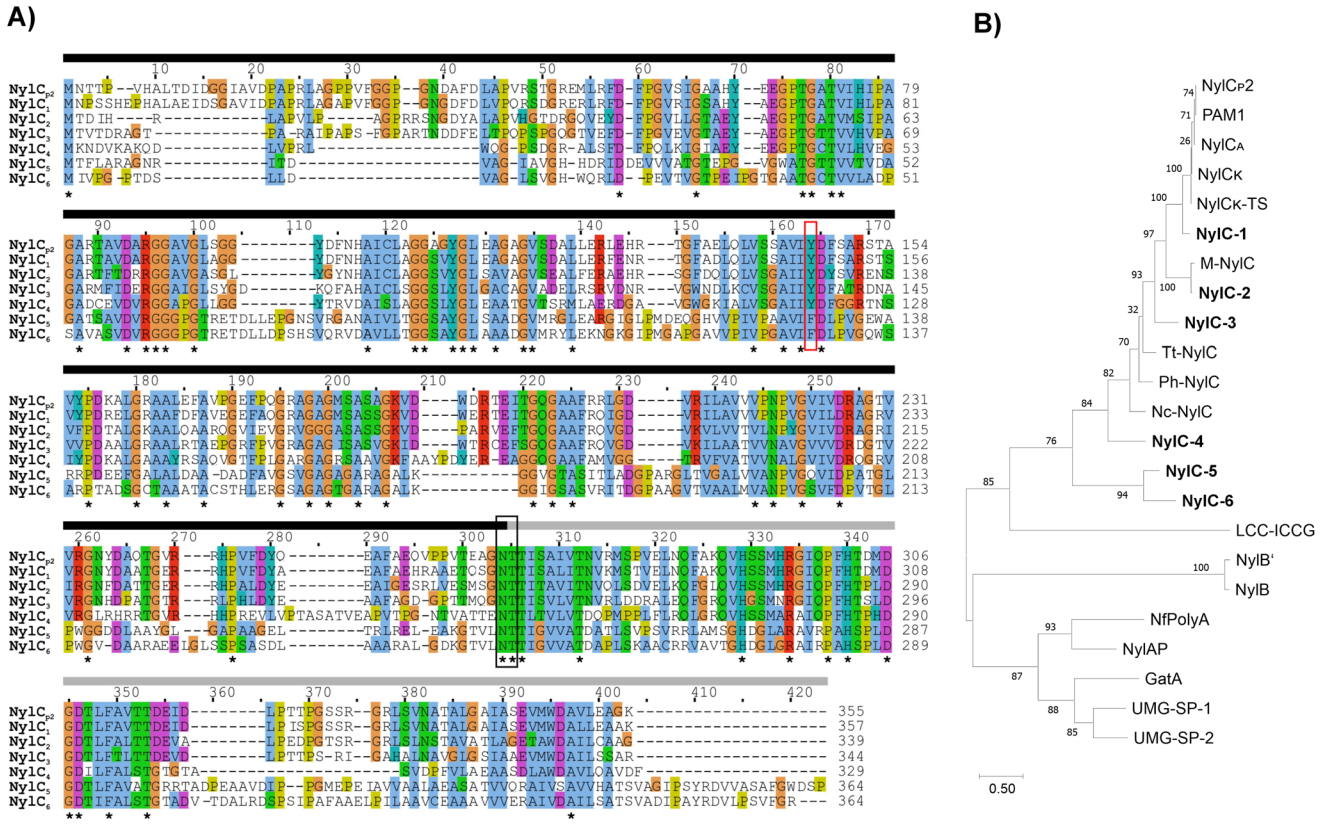

Fig. 1 Multiple sequence alignments and phylogenetic analysis. (A) T-Coffee alignment algorithm[28] was used for the multiple sequence alignment using the EMBL-EBI tool.[29] Amino acids are colored based on Clustal X 2.0 default coloring.[30] Conserved amino acids are indicated with an asterisk (*). The D-D-T catalytic residues (red arrows) and substrate-binding residues (Y/F and K) (orange arrows) are highlighted, while the N/T autocleavage site is enclosed in a black box. The grey and black lines indicate the α- and β-subunits respectively. (B) Phylogenetic tree of NylCs enzyme within the currently known polyamide-active enzymes as described in Bell *et al.*[24] Enzymes described in this study are printed in bold. The tree is drawn to scale, with branch lengths measured in the number of substitutions per site. The percentage of trees in which the associated taxa clustered together are shown next to the branches.

$NylC_{1-6}$ were expressed with a C-terminal His_6-tag allowing their purification. Although the ratio of cleaved (α- and β-subunit) to uncleaved (precursor) $NylC_{p2}$ was reported to increase from approximately 10 to 100% within 48 h of incubation after purification,[19] SDS-PAGE of purified $NylC_{1-6}$ indicated that no significant amounts of precursor protein was present without prior

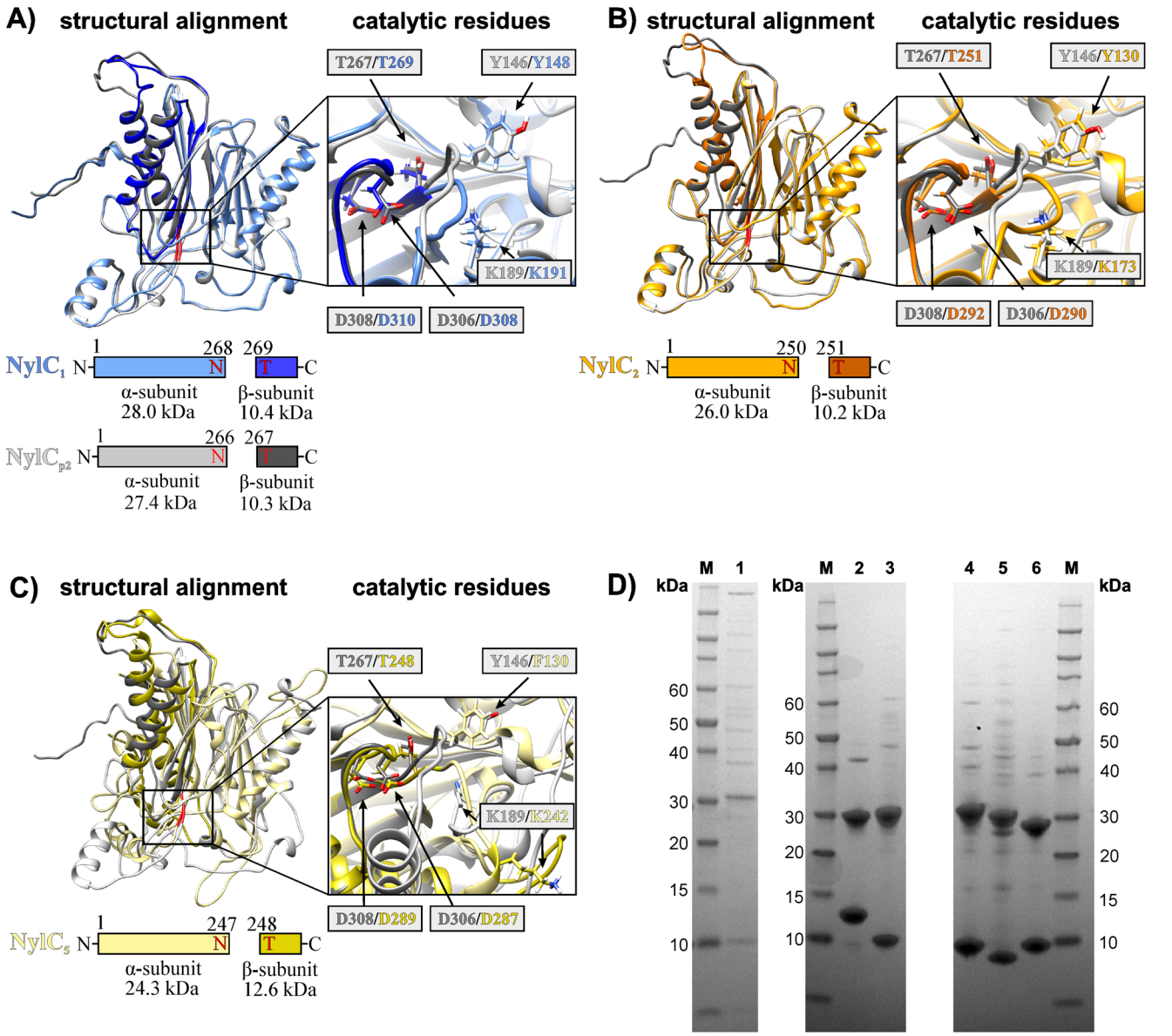

Fig. 2 Structural alignments of $NylC_{p2}$ and $NylC_{1,2,5}$ and enzyme purification. Protein structures of NylCs were predicted using ColabFold[27] and were aligned to $NylC_{p2}$. The holistic structural alignments for $NylC_1$ (A), Nyl C_2 (B) and $NylC_5$ (C) are shown as well as the alignments of the catalytic residues (box). The N/T-autocleavage site is highlighted in red. (D) SDS-PAGE of purified $NylC_{1-6}$. The lanes were loaded as followed: Marker (M), $NylC_1$ (1), $NylC_5$ (2), $NylC_6$ (3), $NylC_3$ (4), $NylC_4$ (5), $NylC_2$ (6). The two bands correspond to the α- and β-subunits.

incubation. Instead, the α- and β-subunits of $NylC_{1-6}$ were detected indicating that their precursor autocleavage might be faster compared to $NylC_{p2}$ (Fig. 1). Moreover, the interaction of α- and β-subunits of $NylC_{1-6}$ were strong enough to allow purification of both subunits with a single C-terminal His_6-tag, which was present in the β-subunits. Unfortunately, $NylC_{p2}$ could not be expressed in *Bacillus* sp. Its heterologous expression seems to be limited to *Escherichia coli* until today.[20,22] For commercial production of nylonases, however, expression in industrial workhorses such as *Bacillus* sp. is a prerequisite, and further optimization would be required.

Activity of $NylC_{p2}$ towards polymeric PA6 was enabled by designing thermostable mutants as elevated reaction temperatures typically result in increased accessibility of amorphous polymer regions due to increased chain mobility.[20,22] To investigate the thermostability and thus evaluate the potential activity towards polymeric substrates, purified $NylC_{1-6}$ were subjected to nano differential scanning fluorimetry (DSF) to determine their melting temperature (T_m). Compared to non-engineered $NylC_{p2}$ (T_m = 52 °C),[21] $NylC_{1-6}$ showed higher thermostabilities ranging from T_m = 58.4 °C ($NylC_1$) to T_m = 82.9 °C ($NylC_4$) (Table 1). The overall higher thermostability indicates that $NylC_{1-6}$ might be active at higher temperatures, which could facilitate depolymerization above the glass transition temperature (T_g) of PA6 (T_g 54 °C). Thermostability is a key factor in enzymatic polymer degradation as extensively

shown for PET.[6,8] Thus, if active, $NylC_{1-6}$ might be promising candidates for enzyme engineering or shuffling to outperform the current thermostability of engineered $NylC_{p2}$ (T_m = 88 °C).[21]

2.2 Activity towards PA6 oligomers

To test whether the $NylC_{1-6}$ candidates are true nylonases, their activities towards cyclic and linear oligomers of PA6, designated as Ahx-oligomers, were tested. Subsequent HPLC analyses were performed to detect degradation products. Although $NylC_{p2}$ was reported to hydrolyze linear and cyclic Ahx-oligomers with a degree of oligomerization greater than three, none of the $NylC_{1-6}$ candidates was active towards soluble linear Ahx oligomers (n = 2–7). Instead, activity towards the cyclic Ahx-oligomer fraction ($n \geq 2$)[31] was detected for $NylC_1$, $NylC_2$, and $NylC_5$ by the release of linear Ahx-oligomers. As additional control reaction, the Ahx-cyclic-dimer hydrolase from *P. ureafaciens* ($NylA_{p2}$)[12] was incubated with the cyclic Ahx-oligomer fraction. As expected, this resulted in the conversion of cyclic Ahx_2 into linear Ahx_2. Activity of $NylC_1$ and $NylC_2$ on the cyclic Ahx-oligomers resulted in the release of linear Ahx_4 and Ahx_5, whereas $NylC_5$ additionally released linear Ahx_3 (Fig. 3A). The linear degradation products were not further hydrolyzed. In contrast to this, $NylC_{p2}$ was reported to further degrade such linear Ahx-oligomers yielding linear Ahx_2 as end-product.[18] Interestingly, no decrease in the concentration of the soluble cyclic oligomers (n = 2–6) could be detected by HPLC, even though linear products were produced by $NylC_1$, $NylC_2$, and $NylC_5$. This may be due to a limitation in the detection of larger, insoluble oligomers. According to this theory, the release of linear Ahx_{3-5} by the NylCs must originate from the hydrolysis of larger insoluble and thus undetectable cyclic oligomers (n > 6). Hence, $NylC_1$ and $NylC_2$ are active towards cyclic Ahx_{8-10}, resulting in the initial ring opening to the corresponding linear oligomers, followed by subsequent degradation to linear Ahx_{4-5} by an endo-cleavage. The additional release of linear Ahx_3 by $NylC_5$, while not degrading cyclic Ahx_6, indicates activity towards cyclic Ahx_7 that is degraded to linear Ahx_{3-4} after initial hydrolysis to linear Ahx_7. To confirm the activity towards exclusively insoluble Ahx-oligomers, only the soluble fraction of cyclic Ahx-oligomers ($n \leq 6$) was tested as substrate for $NylC_{1-6}$ (Fig. 3B) by filtration. Indeed, none of the enzymes showed activity towards the filtered cyclic Ahx-oligomers as no linear degradation products were detected, suggesting that the enzymes were exclusively active on insoluble cyclic and linear oligomers.

Overall, these results reveal that the activity and substrate specificity of $NylC_1$, $NylC_2$, and $NylC_5$ differ from that of

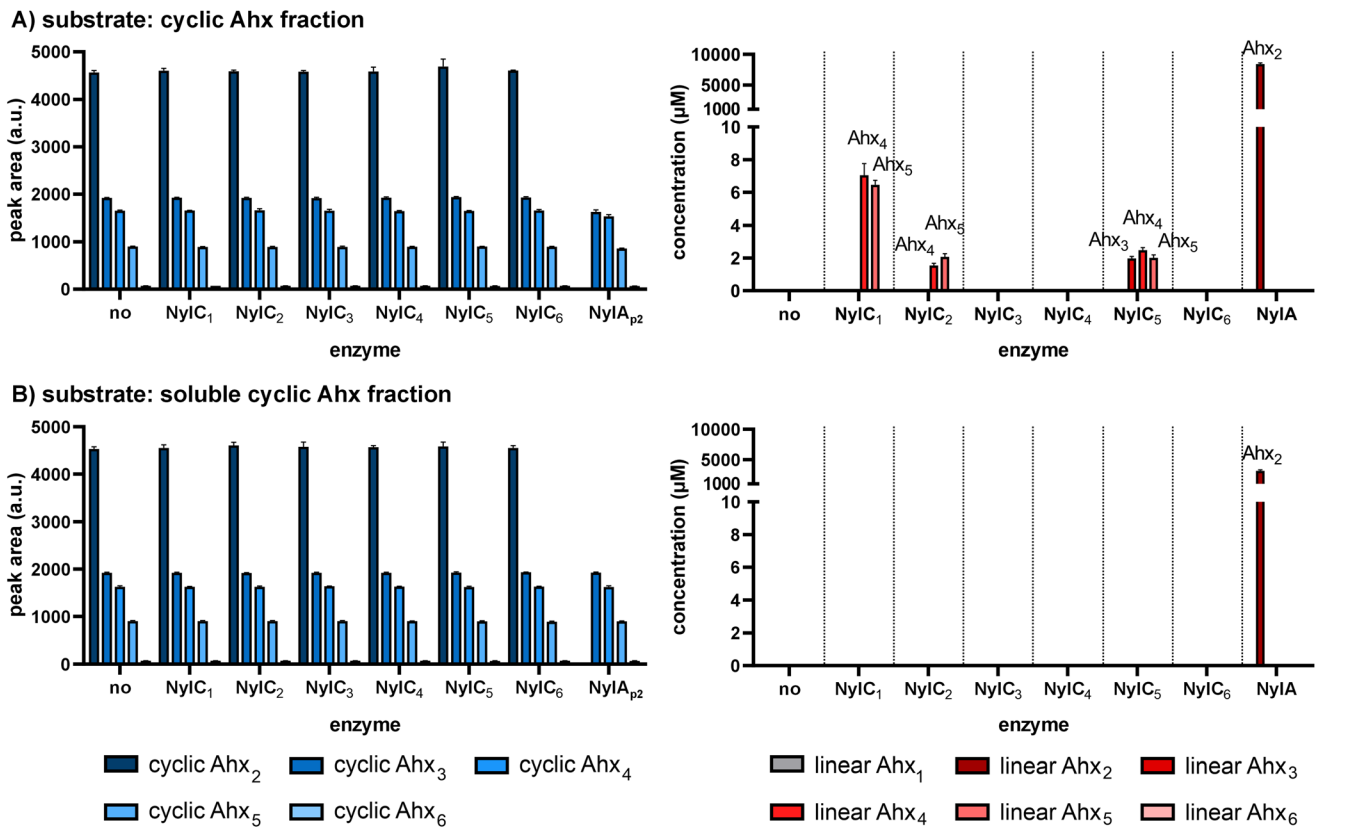

Fig. 3 Activity screenings of $NylC_{1-6}$. Reactions were performed using 4 g L^{-1} cyclic Ahx-oligomers (Aco2)[31] (A) and its soluble fraction that was obtained by filtration (B). Reactions were performed using 500 nM of purified enzyme in 50 mM phosphate buffer, pH 7.3 at 30 °C for 8 h. Cyclic and linear soluble oligomers were detected using HPLC. The mean values and standard deviations (SD) of three replicates are shown (n = 3).

$NylC_{p2}$ as no soluble cyclic or linear oligomers were hydrolyzed by the novel NylC enzymes. Instead, activity towards insoluble oligomers was observed, which might be accompanied by the ability to hydrolyze insoluble linear chains of PA. The inactivity of some NylC candidates highlights the diversity of the N-tn hydrolase superfamily, which complicates the identification of new NylCs based on *in silico* analyses only. The different substrate specificities of the identified NylCs compared to $NylC_{p2}$ and its close homologs indicate a much greater diversity of nylonases in nature than originally anticipated.

The activity of $NylC_1$, $NylC_2$, and $NylC_5$ towards insoluble Ahx-oligomers suggested that they might also be capable of hydrolyzing PA6 of higher molar masses. To test this, each NylC was incubated with powdered PA6 at temperatures between 30 and 70 °C in increments of 10 °C. However, none of the enzymes was active towards PA6 under any of the conditions tested as no soluble oligomers were detected in the supernatants. It has to be noted that the enzymatic activity towards polymeric substrates greatly depends on several factors such as crystallinity and dispersion of the substrate. Previous studies did detect NylC activity on polymeric PA, but they also demonstrated that the activities of NylC are remarkably higher when thin-layered substrate films were used. These films were approximately 1000-fold thinner than the diameter of powdered PA, resulting in a highly increased reaction rate.[20,24] Moreover Nagai *et al.*[20] discovered that even after enzymatic depolymerization of PA6, oligomers were still bound to the polymer chains through hydrogen bonding. The combination of such factors might have contributed to the apparent inactivity of $NylC_{1–6}$ towards powdered PA6 in this study. Enzyme engineering might overcome these barriers as performed for $NylC_{p2}$, whose non-engineered version also showed no activity towards PA6.[20]

2.3 Synthesis and enzymatic degradation of poly(ester amides)

To test the activity of $NylC_{1–6}$ towards other polymeric substrates, we performed activity assays using PEA. In contrast to well-established PA, PEA are an emerging group of polymers and combine the thermal and mechanical properties of PA with the biodegradability of polyesters.[26,32] To investigate if $NylC_{1–6}$ are able to depolymerize PEAs, we tested their activities towards powdered PA6.6-, PA6.10-, or PA6.6-*co*-6.10-based PEAs (PEA1–4) that contained aliphatic or branched diols to yield the desired PEAs (Fig. 5). Both the average molecular weight (M_w) and number average molar mass (M_n) differed among the synthesized statistical PEA ranging from 1846–7371 Da (M_n) and 3587–13 814 Da (M_w), respectively (Table 2). While PEA1 displayed the highest M_n and M_w values among the PEA samples (M_n = 7371 Da and M_w = 13 814 Da), these values still fell significantly below those of PA6 (M_n = 12 220 Da and M_w = 67 860 Da).

The differential scanning calorimetry (DSC) thermograms, showing the heating and cooling curves, revealed crucial thermal properties of PEA1–4 and PA6 (Fig. 4). For PA6, two significantly distinct melting peaks were observed (T_m1 = 213 °C and T_m2 = 220 °C). In contrast, PEA2 and PEA4 showed two similar melting peaks, as both feature the first peak at a temperature of ~173 °C and a second melting peak at 210 °C, which is lower compared to PA6. This phenomenon could be attributed to the characteristics of PEA2 and PEA4 incorporating sebacic acid as a monomer, which increases the stability of secondary crystal structures within the polymer.[33] Notably, the only distinction between PEA2 and PEA4 lies in the ester monomers employed, yet their melting points exhibited similarity. Consequently, it is reasonable to anticipate that the melting point of PEA may be more significantly influenced by the amide regions rather than the ester regions. The existence of two melting peaks may reflect the presence of a secondary crystal structure or the formation of crystals of different sizes,[34] but further investigation is required to define the precise cause. In contrast to PEA2 and PEA4, PEA1 and PEA 3 displayed a less sharp single melting peak at temperatures of 236 °C and 182 °C, respectively. Hence, PEA1 has the highest melting point of all PEA samples. These results suggest that based on the lower melting peaks of the PEA2–4 samples in comparison to PA6, those samples might need to be processed at lower temperatures than PA6, whereas PEA1 might demand a higher processing temperature than PA6.

The DSC thermograms of both PA6 and all PEA samples revealed a recrystallization temperature (T_{rc}) around ~198 °C for PA6, ~208 °C for PEA1, ~188 °C for PEA2 and PEA4, and ~160 °C for PEA3. During cooling, variations in crystal size or type, along with potential defects, may arise in the forming crystalline domains. Upon heating, these smaller crystalline domains (and sometimes defects in the crystal structure) can melt and recrystallize or merge into larger crystalline domains, which subsequently melt at higher temperatures. This recrystallization peak may also indicate the presence of amorphous polymer chains that gain mobility at elevated temperatures, forming a more ordered crystalline structure, as previously documented.[35] In the cooling curve results, PA6 exhibited a

Table 2 Polymer characteristics of PEA1–4 and PA6. Weight average molecular weight (M_w), number average molar mass (M_n) and polydispersity index (PDI) values of unprocessed PEA1–4 and PA6 granules are as well as he melting temperatures (T_m1 and T_m2), re-cooling temperature (T_{rc}), and crystallization temperature (T_c). Data means are with standard deviation (n = 3)

Polymer	M_n (Da)	M_w (Da)	PDI	T_m1 (°C)	T_m2 (°C)	T_{rc} (°C)	T_c (°C)
PA 6	12220 ± 855	67 860 ± 4750	5.55	213 ± 2	220 ± 2	198 ± 2	164 ± 2
PEA1	7371 ± 516	13 814 ± 936	1.87	236 ± 3	—	208 ± 3	200 ± 3
PEA2	2099 ± 147	4174 ± 272	1.99	173 ± 2	210 ± 3	188 ± 3	179 ± 1
PEA3	2139 ± 159	4880 ± 341	2.28	182 ± 2	—	160 ± 2	136 ± 2
PEA4	1846 ± 129	3587 ± 231	1.94	173 ± 2	210 ± 3	189 ± 2	181 ± 3

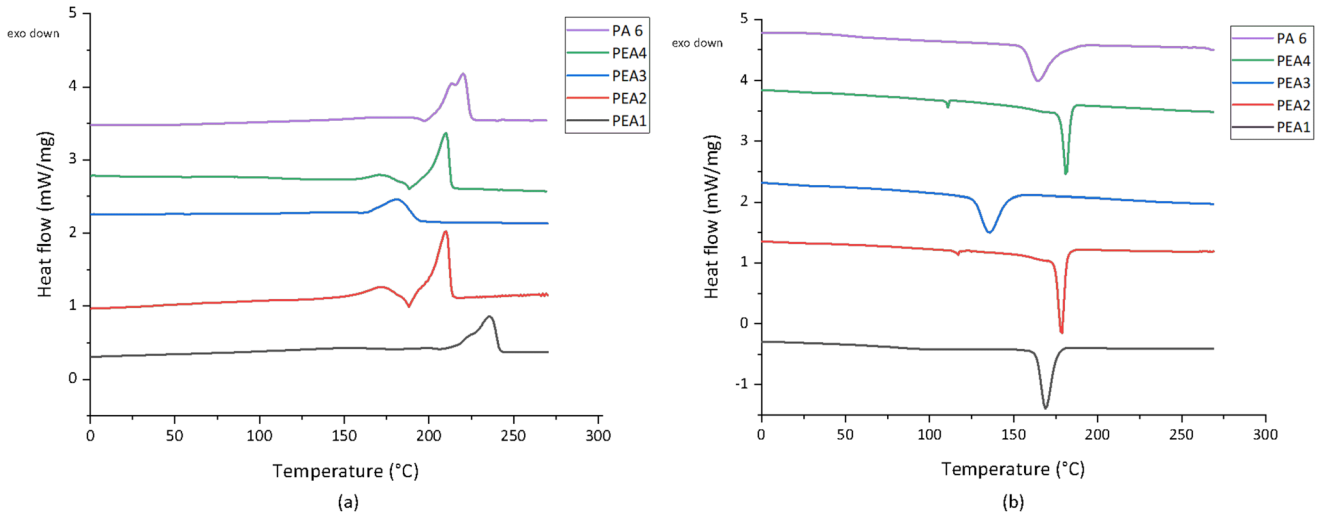

Fig. 4 DSC thermograms of PEA1–4 and PA6 granules. The heating (a) and cooling (b) curves are shown.

crystallization peak remaining at approximately ~164 °C (Fig. 4 and Table 2). Conversely, PEA1, PEA2, and PEA4 displayed peaks at higher temperatures compared to PA6, with respective values of ~200 °C, ~179 °C, and ~181 °C. Only PEA3 exhibited a lower crystallization temperature of 136 °C.

No unambiguous T_g were visible in the DSC data, likely because of the limited sensitivity of the method. However, introducing more variation in the carbon-count of the monomers creates more irregularities in the crystallinity, while it also diminishes the degree of hydrogen bonding between the amide groups. Hence, the T_g of the material should become lower than in PA66 (44 °C (ref. 36)), and PA6 (54 °C (ref. 37)), for example. The relations between nylon composition, hydrogen-bonding, T_g, and T_m were neatly described previously.[33]

After their characterization, the activities of $NylC_{1-6}$ towards PEA1–4 were investigated. $NylC_1$ and $NylC_2$ were active towards PEA1 and PEA3 as the release of linear PA6.6- and PA6.10-oligomers was detected (Fig. 5a and c). $NylC_1$ showed higher activities for both substrates, as it released approximately three-fold more linear PA6.6 dimer ($PA6.6_2$) than $NylC_2$. In contrast to this, no or only low activity was detected towards PEA2 or PEA4, respectively, which contained PA6.10 regions (Fig. 5b and d). These results indicate a preference for $NylC_{1-2}$ towards amide bonds within PA6.6 regions compared to PA6.10 regions. For engineered $NylC_{p2}$, a similar preference for amide bonds consisting of shorter monomers was revealed (PA6.6 and PA6.6-*co*-6.4) and no degradation of PA6.10 has been reported until today.[20] Given the different polymer characteristics of PEA1 and PEA3, the varying biodegradability is likely related to the enzymatic specificities of NylCs rather than to the individual polymer properties of PEA1–4.

To facilitate depolymerization, the well-established leaf and branch compost cutinase (LCC, EC 3.1.1.74, EC 3.1.1.101)[38] able to hydrolyze various polyester, including poly(ester-urethanes),[39] was used for initial depolymerization of the PEAs. Interestingly, Bell *et al.*[6] recently revealed minor activity of an LCC variant towards thin-layered PA6. Here, activity of LCC was expected to release amide oligomers that might be further degraded by $NylC_1$ and $NylC_2$. Since LCC features a high temperature optimum, initial hydrolysis of PEA1–4 was performed at 70 °C and subsequent treatment with $NylC_{1-2}$ was performed at 30 °C. To track any residual activity of LCC during the subsequent incubation at 30 °C, control reactions with $NylB_{p2}$ were performed. This nylonase was reported to specifically hydrolyze linear PA6-oligomers not showing any activity towards PA6.6, PA6.10, and their corresponding oligomers.[13,16] Initial treatment of PEA1–4 by LCC resulted in the release of amide oligomers with primary amino groups revealing activity of LCC towards the amide regions confirming the amidase activity of LCC described by Bell *et al.*[6] (Fig. 5). For PEA1, only containing PA6.6 regions, the release of amide oligomers by LCC was approximately 2.7-fold lower compared to $NylC_1$ (Fig. 5a). In contrast to this, LCC treatment of PEA2–4, containing PA6.6-*co*-PA6.10 or PA6.10 regions, resulted in highly increased amounts of amide oligomers compared to $NylC_1$ (Fig. 5b–d). The combination of LCC and $NylC_1$ resulted in a synergistic effect when PEA1 and PEA3 were tested as substrates, yielding approximately 2.2- and 1.3-fold more soluble products compared to the sum of products released by individual LCC or $NylC_1$ treatments. Hence, initial depolymerization of LCC resulted in the release of larger, undetectable PA6.6-oligomers that were subsequently cleaved by $NylC_1$. This synergistic effect highlights the substrate specificity of $NylC_1$ towards PA6.6-oligomers that were not a preferred substrate for LCC. In contrast to PA6-oligomers, $NylC_1$ was active towards soluble PA6.6-oligomers, as revealed for $PA6.6_4$, which resulted in the formation of $PA6.6_2$ as the end product of hydrolysis. No synergistic effect was observed when PEA2 and PEA4 were tested confirming low activities of $NylC_1$ towards PA6.10-oligomers. Overall, the combination of LCC and $NylC_1$ resulted in the release of approximately 0.6, 0.5, 1,1, and 0.6% of monomer equivalents present in the tested

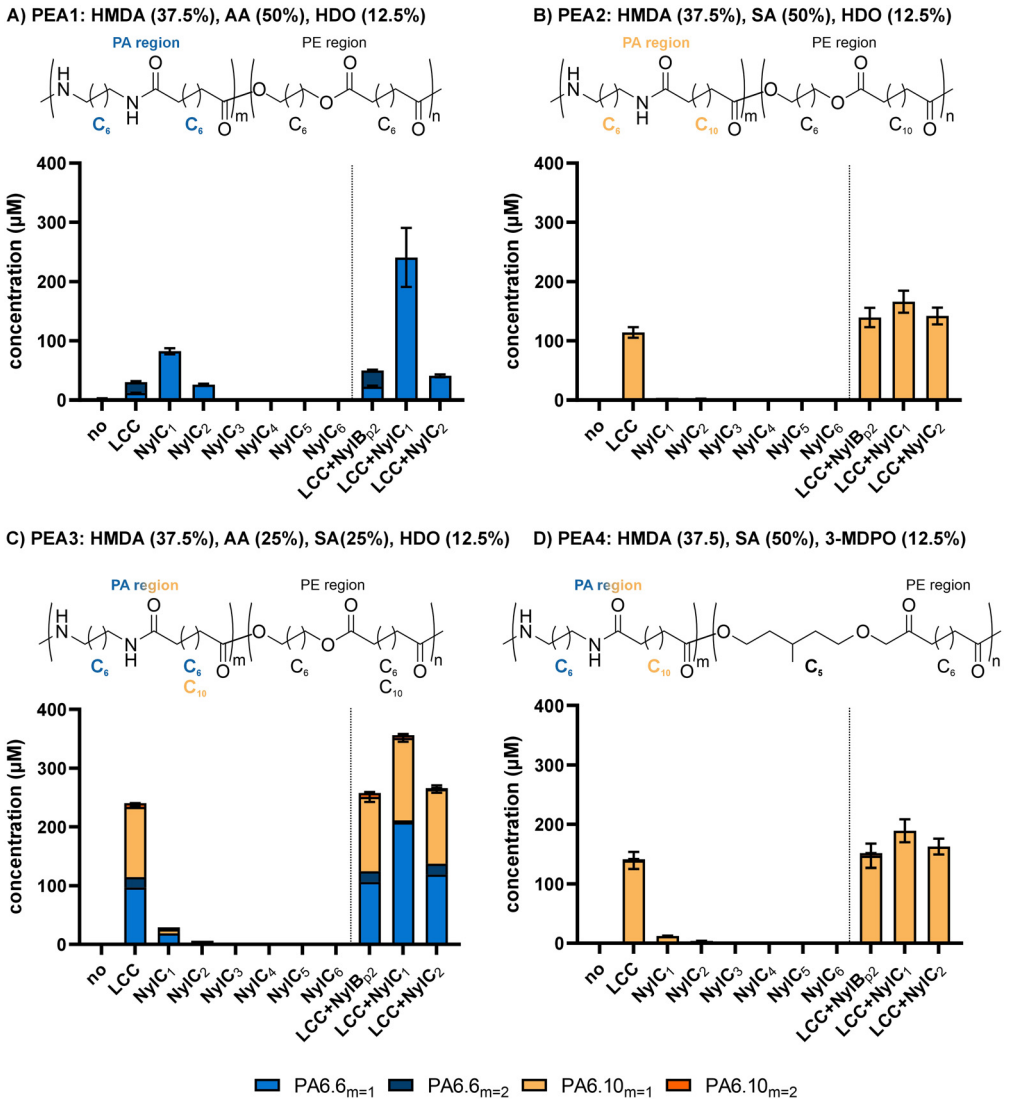

Fig. 5 Enzymatic degradation of PEA by LCC and nylonases. Degradation products containing primary amino groups were detected *via* pre-column derivatization coupled with HPLC analysis. The concentrations of dimer and tetramer of PA6.6 (PA6.6$_{m=1}$ and PA6.6$_{m=2}$) and PA6.10 (PA6.10$_{m=1}$ and PA6.10$_{m=2}$) are shown. Note that a structure of PA6.6 with m = 1 is technically a dimer consisting of one molecule adipic acid and one molecule 1,6-hexamethylenediamine. The composition of PEA being statistical polyester-polyamide copolymer are shown in mol % (HMDA = 1,6-hexamethylenediamine, AA = adipic acid, SA = sebacic acid, HDO = 1,6-hexanediol, and 3-MPDO = 3-methylpentanediol. Powdered PEA (10 g L^{-1})) were used as substrate for the reactions performed in 50 mM phosphate buffer (pH 7.3) using 500 nM of purified enzyme. Reactions containing a single enzyme were incubated at 70 °C (LCC) or 30 °C (NylC$_{1-6}$) for 24 h. For combined enzymatic reactions, samples were first incubated with LCC (70 °C, 24 h) and subsequently with NylC$_1$, NylC$_2$ or NylB$_{p2}$ (30 °C, 24 h). The mean values and standard deviations (SD) of two replicates are shown (n = 2).

PEA1–4 materials respectively. Although the polymer characteristics of PEA2–4 were rather similar, the biodegradability of PEA3 was remarkably higher within this group. This highlights the importance of incorporating PA6.6 regions into PEA as target hydrolysis sites for nylonases. PEA1, containing pure PA6.6-regions, showed less biodegradability compared to PEA3 (PA6.6-*co*-PA6.10 regions) but featured improved polymer characteristics such as increased M_n and M_w. Hence, it is crucial to design future PEA that align both counteracting parameters, as suggested with PEA1, by focusing on the incorporation of PA6.6 regions and boosting the nylonase activities. Overall, NylC$_1$ was revealed as most active nylonase and showed activities towards not only PA6.6 oligomers but also PEA that contain PA6.6-regions (Table 3).

The results from biodegradation experiments support the discussed relations of the T_g of the different materials. The higher degree of mobility of the polymer chains in material with higher monomer variety and, hence, assumed lower T_g supposedly facilitate latching of the enzymes on the polymer chains in a sterical sense, as also indicated in a recent comparison of nylon 66 and nylon 56 biodegradation.[40] Notably, it is reasonable to assume that the T_g of submerged PEAs are considerably lower in the aqueous solution with water molecules interacting with the intramolecular hydrogen bond

Table 3 Comparison of detected enzyme activities. Type of polyamide and oligomeric state to which the enzymes show activity by releasing smaller linear oligomers

Enzyme	Linear oligomers (n^a)	Cyclic oligomers (n^a)
NylC1	PA6 ($n > 6$) PA6.6 ($n \geq 4$)	PA6 ($n > 6$)
NylC2	PA6 ($n > 6$)	PA6 ($n > 6$)
NylC3	No activity	No activity
NylC4	No activity	No activity
NylC5	PA6 ($n \geq 6$)	PA6 ($n \geq 6$)
NylC6	No activity	No activity
NylA	No activity	PA6 ($n = 2$)

[a] n = minimum number of monomers. Enzymes did not show activity to oligomers with less monomers.

network than in the dry polymer,[41,42] further facilitating enzymatic attack.

3 Conclusions and outlook

In the present study, we increased the enzymological diversity of NylCs and discovered three novel NylCs that are active towards insoluble cyclic and linear Ahx-oligomers. Overall, we greatly increased the sequence space of NylCs, facilitating future enzyme engineering to boost their activities towards PA and PEA. $NylC_5$ has only 32% sequence identity to $NylC_{p2}$, with one of the putative substrate binding residues (K242) located in an atypical position. Based on previous engineering of $NylC_{p2}$,[21] rational design can be performed to increase the thermostability of the novel nylonases. Moreover, the recently developed high-throughput screening system for directed evolution of nylonases can be applied to identify yet unknown mutations that increase the overall activities.[22] Such mutations could for example facilitate the post-translational autocleavage, the structural re-assembly of α- and β-subunits, or the interactions between individual NylC monomers. Two of the novel NylCs were active towards polymeric PEA substrates, showing the potential to enable efficient and sustainable enzymatic recycling of PA and PEA in the future. Finally, this study paves the way for linking insights into the enzymatic biodegradability of polymers with their architectural design and highlights PEA as promising hybrid polymers that combine the contrary parameters of performance and biodegradability.

4 Materials and methods

4.1 *In silico* tools

Public and internal databases and genome sequences of isolates were screened for putative NylC candidates by homology searches (threshold ≥30% identity with NylCp). Multiple sequence alignments were performed using the EMBL-EBI tool[29] and the T-Coffee alignment algorithm[28] was used chosen. Amino acids were colored based on Clustal X 2.0 default coloring.[30] The phylogenetic tree construction was conducted using MEGA11[43] by using the Maximum Likelihood method and JTTmatrix-based mode, with 1000 bootstraps. Protein structures were predicted using ColabFold[27] and structural alignments were performed with UCSF Chimera.[44]

4.2 Enrichment cultures

Soil samples (10 g L^{-1}) from a compost heap were used to inoculate mineral salts medium[45] supplemented with 50 g L^{-1} of a poly(ester amide) consisting of adipic acid, 1,6-hexamethylenediamine, and 1,6-hexanediol. Shake flasks were incubated at 30 °C and 200 rpm for 3 d until an increase in turbidity was observed, after which 1% was transferred to fresh medium to enrich strains. After five re-inoculations, enriched strains were isolated on lysogeny broth (LB) agar plates. For cryogenic conservation, strains were cultivated in LB medium for 30 °C for 18 h and 500 μL of cell culture was mixed with 500 μL of 50% (v/v) glycerol. Glycerol stocks were stored at −80 °C.

4.3 16S rDNA sequencing

Genomic DNA was isolated from cells obtained from LB cultures using the Monarch gDNA Purification Kit (NEB). The 16S rDNA sequence was amplified from the isolated gDNA by PCR using Q5 High-Fidelity 2× Master Mix (NEB) and the primer FD1/2 (5′-3′ AGAGTTTGATCMTGGCTCAG) and RP1/2 (5′-3′ ACGGYTACCTTGTTACGACTT).[46] PCR products were purified using a Monarch PCR Cleanup Kit (NEB) and sequenced by Eurofins Genomics (Ebersberg, Germany). The obtained sequencing results were aligned to the nucleotide collection (nr/nt) of the NCBI database using BLASTn.[47]

4.4 Whole-genome sequencing

One microgram of genomic DNA was used for library preparation using the NEBNext Ultra™ II DNA Library Prep Kit for Illumina (NEB). The library was evaluated by qPCR using the KAPA library quantification kit (Peqlab, Erlangen, Germany). Afterwards, normalization for pooling was done and paired-end sequencing with a read length of 2 × 150 bases was performed on a MiSeq (Illumina). The reads of demultiplexed fastq files as the sequencing output (base calls) were trimmed and quality-filtered using the CLC Genomic Workbench software (Qiagen Aarhus A/S, Aarhus, Denmark). The filtered reads were used for *de novo* assembly using the CLC Genomic Workbench software.

4.5 Molecular cloning

Codon-optimized genes encoding the nylonases were chromosomally integrated and expressed in *Bacillus subtilis* using a similar setup as described previously[48] with the following modifications. A 21 bp sequence was added at the terminal gene sequences encoding a C-terminal histidine tag (His_6-tag) and harboring the stop codon. Cells were made competent according to Yasbin *et al.*[49]

4.6 Enzyme purification

Cells of nylonase-expressing *B. subtilis* were cultivated in Cal18 medium (4% Yeast extract, 0.13% $MgSO_4 \cdot 7H_2O$, 5% Maltodextrin, 2% $Na_2HPO_4 \cdot 12H_2O$, 0.67% Na_2MoO_4 trace metal solution and 0.01% Dowfax 63N10)[48] or terrific broth (TB) medium[50] for 48–72 h at 30 °C. Cell cultures were centrifuged at 7000*g* for 15 min and the supernatant was used for immobilized-metal affinity chromatography using His SpinTrap™ columns (Cytivia). After that, cells were desalted with HiTrap® desalting columns (Cytivia) using 50 mM HEPES buffer (pH 7.3). Purified samples were analyzed by SDS-PAGE analysis using Criterion™ Precast Gels.

4.7 Nano differential scanning fluorimetry

The melting temperature (T_m) of the studied enzymes was analyzed by nano differential scanning fluorimetry (nanoDSF) using a Prometheus NT.48 (NanoTemper). For this, the enzymes were diluted to a concentration of 2 mg mL^{-1} in 50 mM HEPES buffer (pH 7.3). The thermal stability was tested with a heating scan range from 20 to 90 °C at a scan rate of 3 °C min^{-1}. Data analyzes and determination of the T_m was performed using the PR ThermControl software (NanoTemper).

4.8 Activity assays

All enzymatic reactions were performed at 30 °C in 50 mM phosphate buffer, pH 7.3 using 500 nM of purified enzyme for 8 h. The cyclic Ahx-oligomer fraction Aco2 ($n \geq 2$)[31] was used at concentrations of 4 g L^{-1} resulting in a turbid reaction sample due to insoluble Ahx-oligomers. For investigating the soluble cyclic Ahx-oligomers as substrate, this mixture was filtered through a 0.22 μm PES filter membrane to remove insoluble oligomers. For degradation experiments with polymeric substrates, 10 g L^{-1} of powdered PEA was used as substrate. Initial treatment with nylonases was performed at 30 °C, whereas LCC treatment was performed at 70 °C. Combined enzymatic degradation was initially performed at 70 °C (LCC) and subsequently at 30 °C after the addition of nylonases.

4.9 High-performance liquid chromatography analysis

Samples obtained from activity assays were filtered through an AcroPrep™ 96-well filter plate (Pall Corporation, Port Washington, NY, USA) to remove any particles prior to HLPC analysis. HPLC analysis was performed using a 1260 Infinity II HPLC equipped with a fluorescence detector (FLD) and a diode array detector (DAD) (Agilent, Santa Clara, California, USA). To analyze linear PA-oligomers harboring primary amine groups, pre-column derivatization using *o*-phthaldialdehyde (OPA) reagent (Sigma-Aldrich, ready-to-use-mix) was performed. For separation of the derivatized molecules, the Kinetex® 2.6 μm EVO C_{18} 100 Å column (100 × 2.1 mm) (Phenomenex, California, USA) was used. As mobile phase, 10 mM sodium-borate buffer (A) (pH 8.2) and methanol (B) was used with an initial ratio of 70 : 30 (A : B).[51] This ratio was gradually increased to 30 : 70 after 10 min and 0 : 100 after 12 min followed by 1 min of 0 : 100. After that, the ratio was switched to 70 : 30 after 14 min and 1 min post-run was performed. The flow was adjusted to 0.4 mL min^{-1} at and the oven temperature was set to 40 °C. Derivatized molecules were detected using a FLD using an excitation of λ = 340 nm and an emission of λ = 450 nm. Detection of cyclic Ahx-oligomers was performed using the DAD with an absorption of λ = 210 nm (reference λ = 300 nm). Cyclic oligomers of Ahx were separated using a Zorbax Eclipse XDB-C8 column (4.6 × 150 mm) with a H_2O_{MilliQ} : MeOH ratio of 60 : 40 and a constant flow of 0.5 mL min^{-1} at 40 °C. As no analytical standards were available for cyclic Ahx-oligomers, the corresponding peak area was analyzed allowing semi-quantitative analysis.

4.10 Polymer synthesis

In a typical random polycondensation procedure, the syntheses of statistical polyester-polyamide (PEA) copolymers from 1,6-hexamethylenediamine, adipic acid or sebacic acid, and 1,6-hexanediol or 3-methylpentanediol (Table 4) were conducted solvent-free and under an inert atmosphere on approximately a 0.15–0.35 kg scale in a glass polymerization reactor (500 mL size; Glasblazerij Janssen B.V.). Mechanical stirring was applied using an overhead stirrer (Heidolph, hei-TORQUE Expert) connected to a magnet stirring coupling piece with a torque restriction of 20 MPa cm^{-1} (Premex Glenfiz), and a 2D-round-shaped stainless steel stirring anchor. Vacuum was applied using a membrane pump (Pfeiffer MVP-15) in conjunction with a manually operated vacuum controller (Vacuubrand, Vacuu-Select). Stoichiometrically correct amounts of reagents (*i.e.* $mol_{diacid} = mol_{diamine} + mol_{diol}$) were weighed into the reactor along with 0.1 wt% catalyst and 0.1 wt% antioxidant. The setup was sealed and carefully purged with five vacuum/nitrogen cycles, and subsequently set at P = 900 mbar. The reaction was initiated by heating using a silicone oil bath to reach 220 °C within 45 minutes under stirring at 50 rpm, upon which the reaction mixture turned into a viscous yellow liquid and profuse water distillation took place. Whenever the water distillation was observed to cease, all reaction conditions were gradually driven more stringent – toward 100 mbar, 240 °C, and stirring at 300 rpm – over the course of two hours. Intermediately, the reactor was filled with nitrogen gas and the flask with aqueous condensate was quickly replaced by an empty one under an outflow of nitrogen gas. The reaction was proceeded for another 3 hours at 240 °C and stirring at 300

Table 4 Composition of PEA in mole percent (mol%). Monomers are abbreviated as followed: adipic acid (AA), sebacic acid (SA), 1,6-hexamethylenediamine (HMDA), 1,6-hexanediol (HDO), and 3-methylpentanediol (3-MPDO)

Polymer	AA	SA	HMDA	HDO	3-MPDO
PEA1	50	0	37.5	12.5	0
PEA2	0	50	37.5	12.5	0
PEA3	25	25	37.5	12.5	0
PEA4	0	50	37.5	0	12.5

rpm but now the vacuum was gradually decreased to 1 mbar to afford substantial buildup of polymer chains, as observed by the thickening of the reaction mixture and the gradual increase of monitored torque on the overhead stirrer. Ultimately, the vacuum was released by nitrogen filling into the reactor, and the polymeric product was cast into a silicone tray while still hot and molten.

4.11 Polymer characterization

Differential scanning calorimetry was carried out using the Q2000 device (TA Instruments, Asse, Belgium). We focused on the melting temperature (T_m), the recrystallization temperature (T_{rc}), and the crystallization temperature (T_c) within the different PEA in comparison to PA6. All samples were tested at a heating rate of 10 °C min^{-1}, using a temperature range of 0 to 275 °C with a sample size of ~5 mg. For each sample, we made three measurements, and the mean values are presented.

The molecular weight of the samples was determined by gel permeation chromatography (GPC) using a 1260 Infinity System (Agilent Technologies, Santa Clara, CA, USA). We used hexafluor-2-isopropanol (HFIP) containing 0.19% sodium trifluoroacetate as the mobile phase, flowing at a rate of 0.33 mL min^{-1}. GPC was used to compare the PEA samples to the polymer PA6. Solutions were prepared by dissolving 3 mg samples in HFIP for ~3 h before passing through a 0.2 μm polytetrafluoroethylene filter and injecting them into a modified silica column filled with 7 μm particles (Polymer Standards Service, Mainz, Germany). The relative molecular weight (M_w), number average molar mass (M_n), and polydispersity index (PDI) were determined using refractive index detectors calibrated with a standard polymethyl methacrylate polymer (1.0 × 105 g mol^{-1}). We performed GPC analysis three times with each sample and presented the mean values for comparison.

Data availability

The data supporting this article have been included as part of the ESI.† Protein sequences are available at NCBI Genbank at https://www.ncbi.nlm.nih.gov/genbank/ through the accession numbers listed in the supplement.

Conflicts of interest

Kenneth Jensen works for Novonesis A/S, a major manufacturer of industrial enzymes. Christian van Slagmaat worked for B4P, a polymer synthesis company, at the time of the study. All other authors have no conflicts to declare.

Acknowledgements

This project has received funding from the Bio-based Industries Joint Undertaking (JU) under the European Union's Horizon 2020 research and innovation programme under grant agreement no. 887711. The JU receives support from the European Union's Horizon 2020 research and innovation programme and the Bio-based Industries Consortium. We gratefully acknowledge Dai-ichiro Kato (Kagoshima University, Japan) for providing cyclic Ahx-oligomers as substrates.

References

1 Textile Exchange, *Preferred Fiber and Materials Market Report*, 2022.
2 A.-J. Minor, R. Goldhahn, L. Rihko-Struckmann and K. Sundmacher, *Chem. Eng. J.*, 2023, **474**, 145333.
3 M. Pietroluongo, E. Padovano, A. Frache and C. Badini, *Sustainable Mater. Technol.*, 2020, **23**, e00143.
4 C. Alberti, R. Figueira, M. Hofmann, S. Koschke and S. Enthaler, *ChemistrySelect*, 2019, **4**, 12638–12642.
5 L. D. Ellis, N. A. Rorrer, K. P. Sullivan, M. Otto, J. E. McGeehan, Y. Román-Leshkov, N. Wierckx and G. T. Beckham, *Nat. Catal.*, 2021, **4**, 539–556.
6 E. L. Bell, R. Smithson, S. Kilbride, J. Foster, F. J. Hardy, S. Ramachandran, A. A. Tedstone, S. J. Haigh, A. A. Garforth, P. J. R. Day, C. Levy, M. P. Shaver and A. P. Green, *Nat. Catal.*, 2022, **5**, 673–681.
7 A. Bollinger, S. Thies, E. Knieps-Grünhagen, C. Gertzen, S. Kobus, A. Höppner, M. Ferrer, H. Gohlke, S. H. J. Smits and K.-E. Jaeger, *Front. Microbiol.*, 2020, **11**, 114.
8 V. Tournier, C. M. Topham, A. Gilles, B. David, C. Folgoas, E. Moya-Leclair, E. Kamionka, M. L. Desrousseaux, H. Texier, S. Gavalda, M. Cot, E. Guémard, M. Dalibey, J. Nomme, G. Cioci, S. Barbe, M. Chateau, I. André, S. Duquesne and A. Marty, *Nature*, 2020, **580**, 216–219.
9 A. Singh, N. A. Rorrer, S. R. Nicholson, E. Erickson, J. S. DesVeaux, A. F. Avelino, P. Lamers, A. Bhatt, Y. Zhang and G. Avery, *Joule*, 2021, **5**, 2479–2503.
10 T. Uekert, J. S. DesVeaux, A. Singh, S. R. Nicholson, P. Lamers, T. Ghosh, J. E. McGeehan, A. C. Carpenter and G. T. Beckham, *Green Chem.*, 2022, **24**, 6531–6543.
11 K. P. Sullivan, A. Z. Werner, K. J. Ramirez, L. D. Ellis, J. R. Bussard, B. A. Black, D. G. Brandner, F. Bratti, B. L. Buss, X. Dong, S. J. Haugen, M. A. Ingraham, M. O. Konev, W. E. Michener, J. Miscall, I. Pardo, S. P. Woodworth, A. M. Guss, Y. Román-Leshkov, S. S. Stahl and G. T. Beckham, *Science*, 2022, **378**, 207–211.
12 S. Kinoshita, S. Kageyama, K. Iba, Y. Yamada and H. Okada, *Agric. Biol. Chem.*, 1975, **39**, 1219–1223.
13 S. Kinoshita, T. Terada, T. Taniguchi, Y. Takene, S. Masuda, N. Matsunaga and H. Okada, *Eur. J. Biochem.*, 1981, **116**, 547–551.
14 S. Negoro, S. Kakudo, I. Urabe and H. Okada, *J. Bacteriol.*, 1992, **174**, 7948–7953.
15 H. Okada, S. Negoro, H. Kimura and S. Nakamura, *Nature*, 1983, **306**, 203–206.
16 S. Negoro, *Appl. Microbiol. Biotechnol.*, 2000, **54**, 461–466.
17 S. Kinoshita, S. Negoro, M. Muramatsu, V. S. Bisaria, S. Sawada and H. Okada, *Eur. J. Biochem.*, 1977, **80**, 489–495.

18 S. Kakudo, S. Negoro, I. Urabe and H. Okada, *Appl. Environ. Microbiol.*, 1993, **59**, 3978–3980.
19 S. Negoro, N. Shibata, D. I. Kato, Y. Tanaka, K. Yasuhira, K. Nagai, S. Oshima, Y. Furuno, R. Yokoyama, K. Miyazaki, M. Takeo, K. Hengphasatporn, Y. Shigeta, Y. H. Lee and Y. Higuchi, *FEBS J.*, 2023, **290**, 3400–3421.
20 K. Nagai, K. Iida, K. Shimizu, R. Kinugasa, M. Izumi, D. Kato, M. Takeo, K. Mochiji and S. Negoro, *Appl. Microbiol. Biotechnol.*, 2014, **98**, 8751–8761.
21 S. Negoro, N. Shibata, Y. Tanaka, K. Yasuhira, H. Shibata, H. Hashimoto, Y. H. Lee, S. Oshima, R. Santa, S. Oshima, K. Mochiji, Y. Goto, T. Ikegami, K. Nagai, D. Kato, M. Takeo and Y. Higuchi, *J. Biol. Chem.*, 2012, **287**, 5079–5090.
22 H. Puetz, C. Janknecht, F. Contreras, M. Vorobii, T. Kurkina and U. Schwaneberg, *ACS Sustainable Chem. Eng.*, 2023, **11**, 15513–15522.
23 K. Yasuhira, Y. Tanaka, H. Shibata, Y. Kawashima, A. Ohara, D. Kato, M. Takeo and S. Negoro, *Appl. Environ. Microbiol.*, 2007, **73**, 7099–7102.
24 E. L. Bell, G. Rosetto, M. A. Ingraham, K. J. Ramirez, C. Lincoln, R. W. Clarke, J. E. Gado, J. L. Lilly, K. H. Kucharzyk, E. Erickson and G. T. Beckham, *Nat. Commun.*, 2024, **15**, 1217.
25 H. Lu, D. J. Diaz, N. J. Czarnecki, C. Zhu, W. Kim, R. Shroff, D. J. Acosta, B. R. Alexander, H. O. Cole, Y. Zhang, N. A. Lynd, A. D. Ellington and H. S. Alper, *Nature*, 2022, **604**, 662–667.
26 M. Winnacker and B. Rieger, *Polym. Chem.*, 2016, **7**, 7039–7046.
27 M. Mirdita, K. Schütze, Y. Moriwaki, L. Heo, S. Ovchinnikov and M. Steinegger, *bioRxiv*, 2021, DOI: **10.1101/2021.08.15.456425**.
28 C. Notredame, D. G. Higgins and J. Heringa, *J. Mol. Biol.*, 2000, **302**, 205–217.
29 F. Madeira, M. Pearce, A. R. N. Tivey, P. Basutkar, J. Lee, O. Edbali, N. Madhusoodanan, A. Kolesnikov and R. Lopez, *Nucleic Acids Res.*, 2022, **50**, W276–W279.
30 M. A. Larkin, G. Blackshields, N. P. Brown, R. Chenna, P. A. McGettigan, H. McWilliam, F. Valentin, I. M. Wallace, A. Wilm, R. Lopez, J. D. Thompson, T. J. Gibson and D. G. Higgins, *Bioinformatics*, 2007, **23**, 2947–2948.
31 S. Negoro, D.-i. Kato, T. Ohki, K. Yasuhira, Y. Kawashima, K. Nagai, M. Takeo, N. Shibata, K. Kamiya and Y. Shigeta, in *Methods in Enzymology*, ed. G. Weber, U. T. Bornscheuer and R. Wei, Academic Press, 2021, vol. 648, ch. 17, pp. 357–389.
32 A. C. Fonseca, M. H. Gil and P. N. Simões, *Prog. Polym. Sci.*, 2014, **39**, 1291–1311.
33 F. Stempfle, P. Ortmann and S. Mecking, *Chem. Rev.*, 2016, **116**, 4597–4641.
34 Y. Furushima, M. Nakada, K. Ishikiriyama, A. Toda, R. Androsch, E. Zhuravlev and C. Schick, *J. Polym. Sci., Part B: Polym. Phys.*, 2016, **54**, 2126–2138.
35 I. Y. Phang, J. Ma, L. Shen, T. Liu and W.-D. Zhang, *Polym. Int.*, 2006, **55**, 71–79.
36 L. T. Lim, I. J. Britt and M. A. Tung, *J. Appl. Polym. Sci.*, 1999, **71**, 197–206.
37 Y. P. Khanna, W. P. Kuhn and W. J. Sichina, *Macromolecules*, 1995, **28**, 2644–2646.
38 S. Sulaiman, S. Yamato, E. Kanaya, J.-J. Kim, Y. Koga, K. Takano and S. Kanaya, *Appl. Environ. Microbiol.*, 2012, **78**, 1556–1562.
39 J. Schmidt, R. Wei, T. Oeser, L. A. Dedavid e Silva, D. Breite, A. Schulze and W. Zimmermann, *Polymers*, 2017, **9**, 65.
40 K. Luo, J. Liu, K. Abbay, Y. Mei, X. Guo, Y. Song, Q. Guan and Z. You, *Polymers*, 2023, **15**(13), 2877.
41 H. K. Reimschuessel, *J. Polym. Sci., Polym. Chem. Ed.*, 1978, **16**, 1229–1236.
42 W. G. Perkins and R. S. Porter, *J. Mater. Sci.*, 1977, **12**, 2355–2388.
43 K. Tamura, G. Stecher and S. Kumar, *Mol. Biol. Evol.*, 2021, **38**, 3022–3027.
44 E. F. Pettersen, T. D. Goddard, C. C. Huang, G. S. Couch, D. M. Greenblatt, E. C. Meng and T. E. Ferrin, *J. Comput. Chem.*, 2004, **25**, 1605–1612.
45 N. J. P. Wierckx, H. Ballerstedt, A. M. de Bont Jan and J. Wery, *Appl. Environ. Microbiol.*, 2005, **71**, 8221–8227.
46 W. G. Weisburg, S. M. Barns, D. A. Pelletier and D. J. Lane, *J. Bacteriol.*, 1991, **173**, 697–703.
47 E. W. Sayers, E. E. Bolton, J. R. Brister, K. Canese, J. Chan, D. C. Comeau, R. Connor, K. Funk, C. Kelly, S. Kim, T. Madej, A. Marchler-Bauer, C. Lanczycki, S. Lathrop, Z. Lu, F. Thibaud-Nissen, T. Murphy, L. Phan, Y. Skripchenko, T. Tse, J. Wang, R. Williams, B. W. Trawick, K. D. Pruitt and S. T. Sherry, *Nucleic Acids Res.*, 2022, **50**, D20–D26.
48 K. Jensen, P. R. Østergaard, R. Wilting and S. F. Lassen, *BMC Biochem.*, 2010, **11**, 47.
49 R. E. Yasbin, G. A. Wilson and F. E. Young, *J. Bacteriol.*, 1975, **121**, 296–304.
50 Cold Spring Harbor Laboratories, *Cold Spring Harb. Protoc.*, 2015, DOI: **10.1101/pdb.rec085894**.
51 R. Zuchowski, S. Schito, F. Neuheuser, P. Menke, D. Berger, N. Hollmann, S. Gujar, L. Sundermeyer, C. Mack, A. Wirtz, O. H. Weiergräber, T. Polen, M. Bott, S. Noack and M. Baumgart, *Microb. Cell Fact.*, 2023, **22**, 71.